Design of an Ankle Rehab Robot With a Compliant Parallel Kinematic Mechanism

Nishant Jalgaonkar[1]
Precision Systems Design Laboratory,
Mechanical Engineering,
University of Michigan,
Ann Arbor, MI 48109
e-mail: nishjal@umich.edu

Adam Kim
Precision Systems Design Laboratory,
Mechanical Engineering,
University of Michigan,
Ann Arbor, MI 48109
e-mail: akmkim@umich.edu

Shorya Awtar
Precision Systems Design Laboratory,
Mechanical Engineering,
University of Michigan,
Ann Arbor, MI 48109
e-mail: awtar@umich.edu

In this article, we present the design of a novel ankle rehabilitation robot (ARR), called the Flex-ARR, that employs a compliant parallel kinematic mechanism (PKM) with decoupled degrees-of-freedom. While multiple ARRs have been developed and commercialized, their clinical adoption has been limited primarily because they do not emulate the natural motion of the ankle. Based on a review of existing ARRs and their limitations, this article defines functional requirements and design specifications for an optimal ARR. These are then used to develop a design strategy followed by conceptual and detailed design of a novel ARR. The proposed Flex-ARR is designed to collocate the biological center of rotation of the ankle with that of the robot's center of rotation to allow natural ankle motion. The strategic use of a compliant PKM in the Flex-ARR not only absorbs any residual misalignment between these two centers but also helps inherently accommodate variations in user foot sizes with minimal adjustments. Detailed design includes the ARR structure with adjustable features, compliant PKM optimization, sensor and actuator selection, and an alignment tool. [DOI: 10.1115/1.4050103]

Keywords: ankle rehab robot, compliant mechanism, ankle rehabilitation, medical robotics

1 Background and Motivation

The ankle is a complex joint connecting the leg region of the lower limb to the foot and allows for daily activities like maintaining balance and walking [1,2]. Figure 1 shows the ankle with its associated axes, center of rotation (CoR), and motions. The ankle supports large loads (~3 to 6 kN) during activities like walking and running. Not surprisingly, it is the site of many musculoskeletal injuries that require rehabilitation such as sprain injuries and ligament injuries [2]. In addition to musculoskeletal injuries, the ankle also requires rehabilitation in cases of neurological disorders/injuries such as cerebral palsy and stroke leading to a loss of motor control or drop foot [3,4]. Rehabilitation therapy (also known as simply *rehab*) plays a vital role in the treatment of said injuries [2].

Typically, rehab for musculoskeletal ankle injuries involves passive/active range-of-motion (RoM) and muscle strengthening exercises. Therapists use manual exercise, free weights, and specialized passive devices such as balance boards and resistance bands to conduct rehab [5]. Stroke neurorehabilitation usually requires additional task-specific movement training to promote motor recovery, e.g., by using a gait training robot to mimic walking gait of the patient [6]. Across the various forms of rehab, therapists find it challenging to conduct exercises in a repetitive and precise manner to ensure consistency of treatment. Repetitive manual exercises often fatigue the therapist and can potentially impact the quality of treatment. Therapists also need to assess the patient's ankle during the course of therapy. They may conduct this assessment using tools such as a goniometer (for range of motion) or a dynamometer (for muscle strength), and they often use their own subjective judgment for such evaluation [7–11].

Robotic devices for rehabilitation have been proposed to address these challenges for several reasons: (a) robots can be designed to provide a wide range of repetitive therapy exercises in a precise manner without tiring the therapist and (b) robots can employ multiple sensors to capture accurate quantitative data about the ankle that can be used to provide objective assessment and therapy decisions [2,7,12–14]. While several robots have been proposed for ankle rehabilitation, as summarized in Sec. 2, the following limitations in the design and performance of existing ankle rehabilitation robots (ARRs) have been identified in the literature [7,15]:

(1) *The ARRs do not adequately emulate the natural motion of the ankle*, i.e., allow the patient to move their ankle as they naturally would. The negative consequences of not emulating natural ankle motion include reaction torques at the ankle and/or unnatural compensatory motion of the patient's lower limb joints (i.e., knee or hip). The unnatural motion of the ankle is in response to the misalignment of the biological center of rotation (B-CoR) of the ankle and the robot center of rotation (R-CoR), which interferes with the therapy [15,16].
(2) *An inability of ARR to adapt to the highly varying individual needs of the patients* who present with large variations in the size and the shape of their lower limb. This variation includes varying RoM, muscle strength, axis and center of rotation. These variations make the setup and use of the ARR by a physical therapist more onerous.

To address these limitations in existing ARR, we present the design of a novel ARR, called the Flex-ARR (Fig. 2), which uses a compliant parallel kinematic mechanism (PKM) to provide two decoupled degrees-of-freedom (DoF); plantarflexion/dorsiflexion

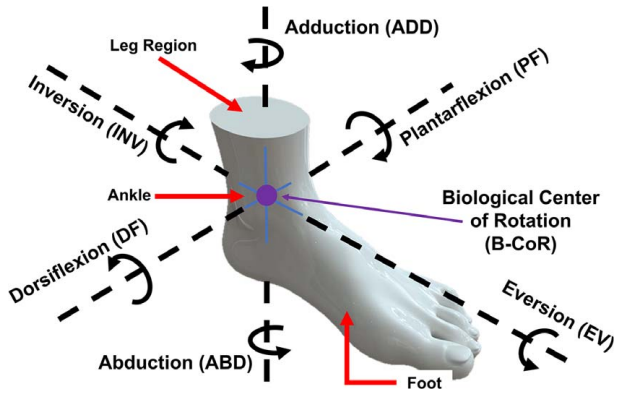

Fig. 1 Ankle axes, center of rotation, and motions

[1]Corresponding author.
Contributed by the Mechanisms and Robotics Committee of ASME for publication in the Journal of Mechanisms and Robotics. Manuscript received September 28, 2020; final manuscript received January 22, 2021; published online April 9, 2021. Assoc. Editor: Philip A. Voglewede.

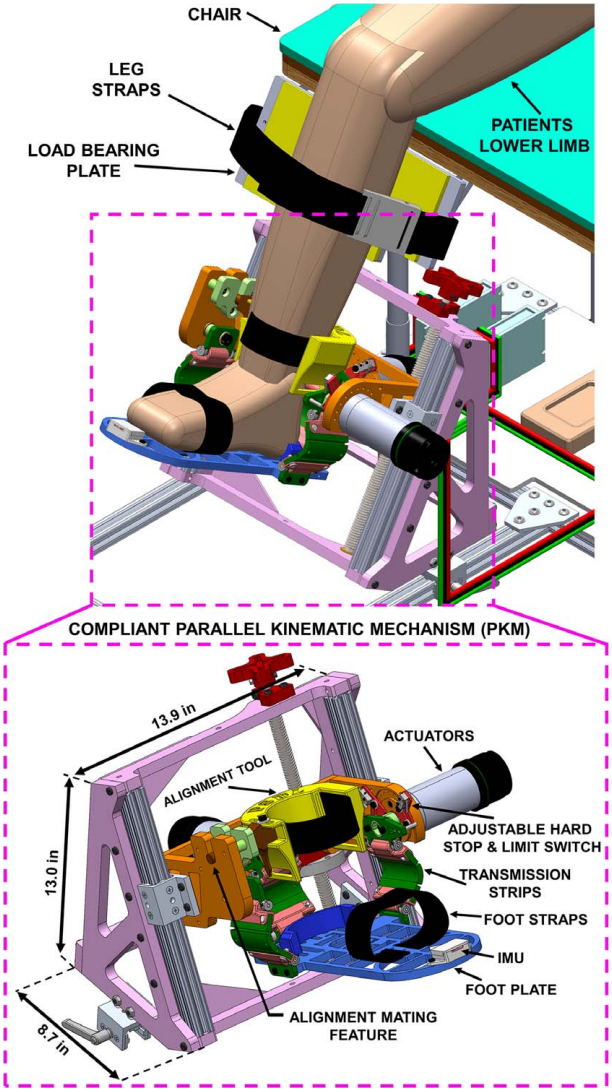

Fig. 2 Proposed Flex-ARR full system CAD

(PF/DF), and inversion/eversion (INV/EV) rotations of the ankle. This compliant PKM is designed with appropriate compliance along its degrees of constraint (DoC) to absorb minor misalignment of the B-CoR and R-CoR and allow for natural ankle motion. The PKM also allows the Flex-ARR to inherently accommodate for variations in patient's lower limb dimensions without the need for onerous adjustment features. The Flex-ARR includes a novel pre-therapy alignment tool that allows the therapist to locate the B-CoR, while the patient is seated or laying down on an examination bed before strapping the patient to the Flex-ARR, thereby allowing better view and access. Existing ARRs rely on visual alignment between the B-CoR and the R-CoR [17], which is not only challenging for the therapist but also prone to misalignment errors.

The remainder of this article is organized as follows. A detailed review of existing ARRs is presented in Sec. 2. Through an assessment of current ARRs limitations, ankle biomechanics, and therapist needs, a list of functional requirements (FRs) and design specifications are compiled in Sec. 3. A design strategy to address these requirements and specifications and resulting concept generation is presented in Secs. 4 and 5, respectively. The detailed design of the Flex-ARR including PKM optimization, actuator and sensor selection, and overall structural design and adjustability are covered in Sec. 6. Future work that includes fabrication and testing is discussed in Sec. 7.

2 Review of Commercial and Research Ankle Rehabilitation Robots

ARRs can be categorized into two functional types—wearable and platform [2,7,18]. Wearable ARRs such as exoskeletons for rehab [19] comprise a customizable anthropomorphic user interface for reinforcement and corrective training procedures [2,7,8]. Platform ARRs comprise a mobile plate that transmits motion and forces to the patient's foot and is connected to a static base [7,20] via a mechanism. Platform ARRs are most commonly used in physical therapy clinical settings and are typically designed to control the INV/EV and PF/DF motion of the ankle [2,7]. They are used in rehab to improve the RoM of the ankle, avoid ankle stiffness, and improve muscle strength. This article focusses on platform ARRs as they remain an unsolved challenge in the field of rehab robotics and meet a wider range of needs for the therapist.

Table 1 and associated Fig. 3 provide a summary of various existing platform ARRs in the research literature. Typically, platform ARRs implement PKMs [2,7,18] between the mobile plate and the static base as opposed to serial kinematic mechanisms due to the former's multi-DoF capability in a compact form factor and high stiffness [21]. In the literature, it has been proposed that the misalignment between the ARRs center of rotation (R-CoR) and the B-CoR is responsible for preventing natural motion of the ankle [7,15,25]. Most PKMs in existing ARRs present kinematic or accessibility limitations in their ability to align their R-CoR with the B-CoR of the patient's ankle. These ARRs either have R-CoRs that do not remain stationary [20,26,29] or have R-CoRs that are fixed but present practical challenges in being able to collocate them with the B-CoRs of different patients before and during rehab when exercises are conducted over the RoM of the ankle [24,25].

The ARRs presented in Figs. 3(*a*), 3(*b*), 3(*d*), and 3(*f*) have a fixed R-CoR and provide enough space for the patient's foot to interface with the ARR. These ARRs leverage different types of mechanisms with the goal of providing an R-CoR that can be collocated with the B-CoR. However, the ankle, while often modeled as a perfect spherical joint, has axes of rotations (and

Table 1 Selection of representative ARRs from the literature review

Author (robot name)	Year	DoF	Robot RoM (deg)		Type of training
			PF/DF	INV/EV	
Li et. al. [21] (PARR), Fig. 3(*a*)	2020	3	42/26	16/16	CPM, assistive, resistance
Kumar et. al. [22]	2019	6	37/20	35/15	—
Zhou et. al. [23], Fig. 3(*e*)	2015	1	—	—	Proprioceptive evaluation
Jamwal et. al. [15], Fig. 3(*b*)	2014	3	46/46	26/26	CPM, resistance
Saglia et. al. [14] (ARBOT), Fig. 3(*c*)	2009, 2013	2	15–20	—	CPM, assistive, resistance
Wang et. al. [24]	2013	3	50/50	30/30	—
Malosio et. al. [25] (PKAnkle), Fig. 3(*f*)	2012	3	—	—	CPM
Yoon and Ryu [26]	2005	4	50/50	55/55	CPM, resistance, balance
Girone et. al. [20] (Rutgers Ankle), Fig. 3(*h*)	2001	6	45/45	40/40	CPM, resistance

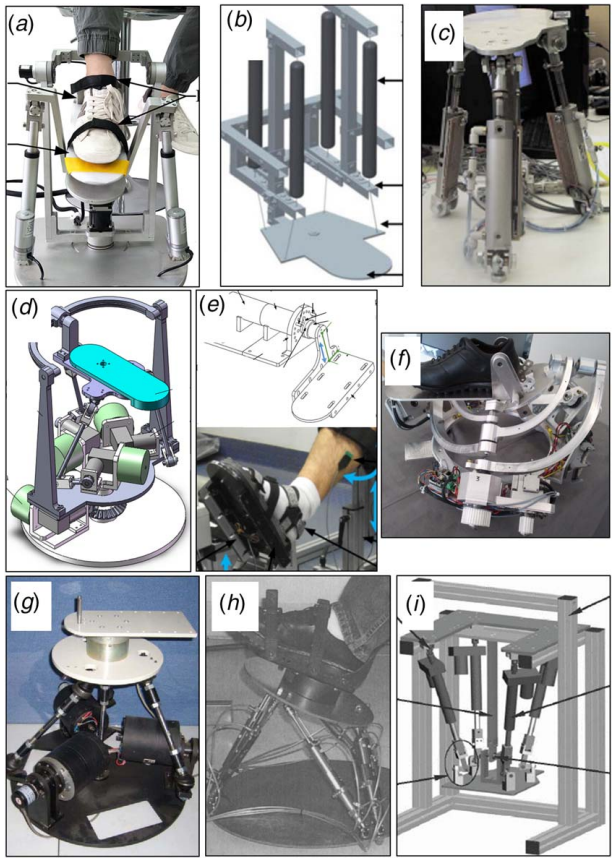

Fig. 3 (*a*) Parallel ARR [21], (*b*) pneumatic muscle actuator-based ARR [15], (*c*) Ref. [14], (*d*) Ref. [24], (*e*) proprioception ARR [23] (Reprinted with permission from Elsevier © 2015), (*f*) modified agile eye ARR [25], (*g*) Ref. [27], (*h*) Stewart platform derivative [20] (Reprinted with permission from Springer Nature © 2001), and (*i*) Ref. [28]

associated B-CoR) that move throughout its RoM [1,30,31]. As a result, existing ARRs with fixed R-CoRs are unable to address the CoR misalignment throughout the RoM of the ankle since the mechanisms are generally too stiff in their constraint directions. Recognizing these limitations, some researchers have used surface electromyography to track unfavorable muscle activation to identify misalignment [32]. This provides further evidence that compensatory motion of lower limb (such as knee or hip) is indicative of unnatural ankle motion.

The ARRs in Figs. 3(*c*) and 3(*g*) have a central strut with a universal joint at the end that connects to the mobile plate to provide the DoF and DoC. However, the universal joint of the central strut places the R-CoR below the moving plate, and it is impossible to collocate it with the B-CoR of the ankle. The ARR presented in Fig. 3(*h*) (Rutgers Ankle) has 6 DoF and a virtual CoR that can be controlled. To collocate it with the B-CoR requires perfect tracking of the patients B-CoR, which poses practical challenges and increases control complexity [14,15,27].

Several commercial platform-type ARRs were also investigated [33], and it was found that while the weight and overall dimensions of the robots vary, the key performance capabilities do not. Most commercial ARRs include the PF/DF and INV/EV range of motion of the robot. User interfaces are explicitly integrated into all of the commercial ARRs with ergonomic considerations made for lower limb restraints (e.g., straps) and the ability to adapt to varying lower limb dimensions [34–38]. However, they do not address the need of reducing or accommodating the misalignment of the R-CoR and B-CoR and often require numerous adjustments.

In addition to the limitations of the ARR mechanisms in providing an R-CoR that can be collocated with the B-CoR, most ARRs (research and commercial) rely on visual determination of the B-CoR and its alignment with the R-CoR by the therapist during initial setup. The therapist first uses their skill and judgment to visually determine the B-CoR of the patient, and then second, they attempt to collocate it with the R-CoR of the ARR. This process has the potential for error in both steps—an attempt by experts to identify the B-CoR using sight can lead to an error as high as 9 mm [17]. This error is compounded by the second step, and there is no data available on the error involved in visually aligning a point on the patient's ankle with the R-CoR of the ARR. This serves as motivation for an alignment tool as part of the platform ARR, in addition to an appropriate ARR mechanism, to ultimately ensure natural ankle motion.

A more detailed discussion of the platform ARRs found in the literature and commercial products is presented in Ref. [27]. In summary, the need for an ARR that allows for natural ankle motion by the alignment of R-CoR and B-CoR over the entire range of motion and that meets the needs of a broad population with varying physiology remain unsolved. Based on this review of the literature, a list of functional requirements for the design of an optimal platform ARR were generated.

3 Functional Requirements for Ankle Rehabilitation Robot

Based on an assessment of existing ARRs, their limitations, and the needs of therapists, several system level FRs for an optimal platform ARR are proposed:

FR1—Adequate DoF: The optimal ARR should provide at least two rotational DoFs, specifically to allow for controlled rotation in PF/DF and INV/EV. These motions are used in everyday activities

Table 2 ARR technical specifications

FR	Specifications	Target value	Notes	Flex-ARR performance
FR1	RoM in PF/DF (deg)	±25	Values vary in literature, a representative sample was chosen [1,39]	±25 (verified by CAD)
FR1	RoM in INV/EV (deg)	±15		±20 (verified by CAD)
FR1	Peak speed (deg/s)	>23	This was determined based on motion profile estimation	42 (actuator datasheet)
FR1	Peak resistance torque of ankle (Nm)	>25	Based on passive ankle stiffness model, at max PF position [40]	30 (actuator datasheet)
FR4	Position resolution (deg)	~1	5x improvement on Goniometer [9,10]	0.09 (encoder resolution)
FR4	Torque Resolution [Nm]	~0.1	Benchmarked to dynamometer [41]	0.1 (motor driver current resolution)
FR3	Misalignment between B-CoR and R-CoR	<5 deg <7 mm	Based on current ARRs misalignment est. [17]	See Sec. 6.1
FR2	Foot length (in.)	<12	Based on data of US population [42]	12 (foot plate length is 13)
FR2	Foot width (in.)	<4		5 (foot plate width is 6)
FR2	Lower limb length (m)	~0.78	Mean limb lengths [43]	See Sec. 6.3

such as walking, and hence, therapists focus on these motions during therapy.

FR2—Customizable to Individual Patients: The ARR should be able to accommodate a broad spectrum of patients, given their varying dimensions of the lower limb, foot, or type of injury while requiring minimal adjustments.

FR3—Natural Ankle Motion: The ARR should provide no kinematic or accessibility limitation to the natural motion of the patient's ankle. We postulate that to promote natural ankle motion, the ARR should absorb any misalignment (translational and angular) between the B-CoR and R-CoR throughout the rehab (i.e., both at initial setup and during rehab exercise).

FR4—Multiple Therapy Modes: The ARR should have multiple therapy modes, i.e., continuous passive motion (CPM) and muscle strengthening (resistance therapy). The ARR must also provide multiple quantitative measurements to assess the health of the ankle such as its RoM, joint speed, muscle strength, and muscle proprioception.

FR5—Safety and Ergonomics: The ARR should be safe for the patient and therapist to use. The ARR should include multiple, redundant safety measures to prevent any injury and pain to the patient and also ensure that there are no obstructions to the therapist performing therapy.

The functional requirements qualitatively capture the problem scope and definition, Table 2 provides the corresponding quantifiable technical specifications for an optimal ARR.

4 Proposed Design Strategy for Ankle Rehabilitation Robot

Based on the aforementioned FRs and technical specifications, a design strategy for ARRs was developed. The optimal ARR is decomposed into individual modules or subsystems, as shown schematically in Fig. 4. The platform ARR will have a frame module, which will serve as the 'reference ground' for the PKM module to provide DoFs to the moving plate. In addition, the frame module will be load bearing and will bear the weight of the PKM, actuators, sensors, patient's lower limb, etc. The patient's leg region will be attached to the ARR frame. The foot has DoF with respect to the leg region, and if the ARR mechanism shares this ground, its DoFs can be aligned with those of the foot more easily.

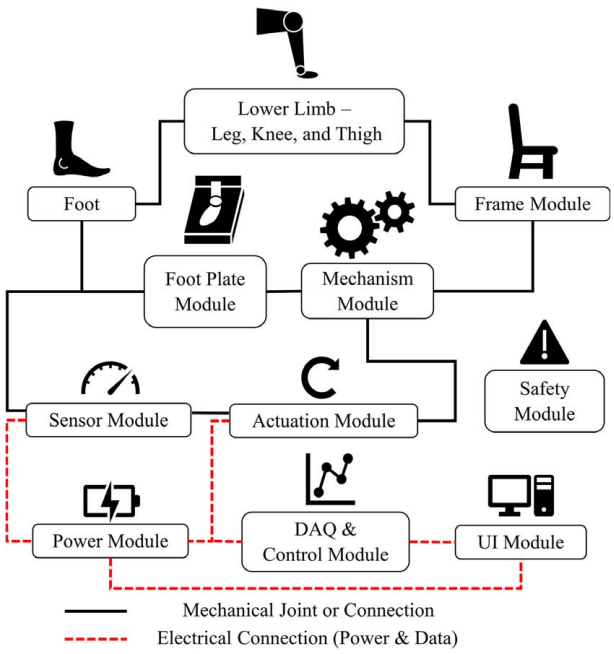

Fig. 4 Schematic of the proposed design strategy for ARR

Per FR1, the optimal ARR mechanism should have at least 2 DoF, and as per FR2, it should be able to adapt to individual patient needs. Ideally, all of this should be accomplished by the mechanism module. The mechanism should produce a virtual center of rotation (the R-CoR) between the foot plate module and the frame module and leave enough physical space for a patient to insert their foot into the foot plate module such that their B-CoR can be collocated with the R-CoR and absorb any misalignment between the CoRs. This will address FR3. The foot plate module of the ARR will be the interface of the ARR with the patient's foot. Upon actuation, the mechanism should impart motion to the foot module, and the foot module will convey that motion to the patient's foot and ankle.

Per FR4, the optimal ARR should have an actuation module to actuate the mechanism to provide therapy, and a sensor module to provide objective quantitative measurements of ankle health parameters such as RoM, speed, and muscle strength. As per FR5, the proposed ARR would require a user interface for the therapist to control its operation and an interface for the patient for the purpose of evaluation (i.e., proprioception evaluation) and for safety (i.e., safety stop). To ensure the safety of the patient and therapist, the ARR should also comprise a safety module, mechanical hard stops, emergency stop buttons, and software-based limits.

Finally, the ARR should comprise a Data Acquisition & Control module to control the DoFs of the PKM in the various therapy modes and to collect the data required by the ARR and the therapist for patient assessment. A Power module provides electrical power to other modules of the system. On the basis of this proposed design strategy, we proceed to further conceptualize and develop a novel ARR with the objective of meeting all FRs listed in Sec. 3.

5 Concept Generation and Preliminary Design

Based on the functional decomposition provided by the aforementioned design strategy, multiple concepts were generated for each module. Special emphasis was given to the design of the mechanism module. Concept generation began with the most promising designs from the literature—modified agile eye [25] and gimbal [24] inspired mechanisms. These designs came closest to meeting all FRs defined earlier except FR3, which specifically pertain to mechanism performance. These ARRs are unable to absorb misalignment of CoRs to provide natural ankle motion. In addition, those ARRs did not provide intuitive alignment features for the therapist to use to collocate the B-CoR and R-CoR. To overcome these challenges, it was concluded that if finite compliance is introduced in the constraint directions (i.e., DoC) of the mechanism, it can alleviate any conflict between the CoRs. That kind of mechanism will allow the ARR to absorb any misalignment between the R-CoR with the B-CoR.

A broader survey of mechanisms that provide at least two rotational DoF [44] and features that meet the relevant FRs led to compliant PKMs, in particular to the FlexDex mechanism shown in Fig. 5. The FlexDex mechanism [44–46] creates a 2 DoF joint with a virtual CoR projected in an open space. As a result, this CoR can be collocated with the CoR of a human articulation joint without obstructing the natural motion of the latter. Because of the compliant transmission strips, the FlexDex mechanism can inherently accommodate variations in the user size, which effectively reduces the need for adjustment features. This mechanism also decouples the two rotational DoF, which makes actuation, transmission, and control easier.

In Fig. 6, the detailed view of the proposed Flex-ARR foot plate and associated compliant PKM are shown. The figure shows the axis for PF/DF rotation, the INV/EV rotation, and the vertical axis that corresponds to the rotational DoC of the PKM. In addition, the figure shows the R-CoR as a dot and worst-case misalignment for the B-CoR. The compliant transmission strips are a key to the design and operation of this mechanism. The transmission strips have pin joints on either end. One pin joint connects to the actuator

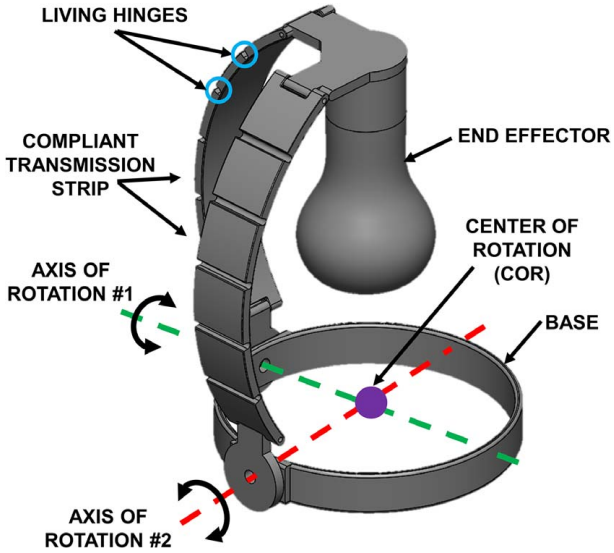

Fig. 5 Compliant PKM of the FlexDex device [44–46]

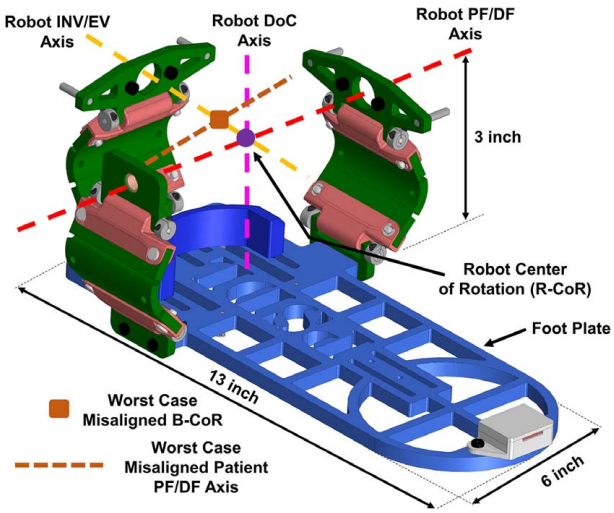

Fig. 6 Flex-ARR foot plate and compliant PKM

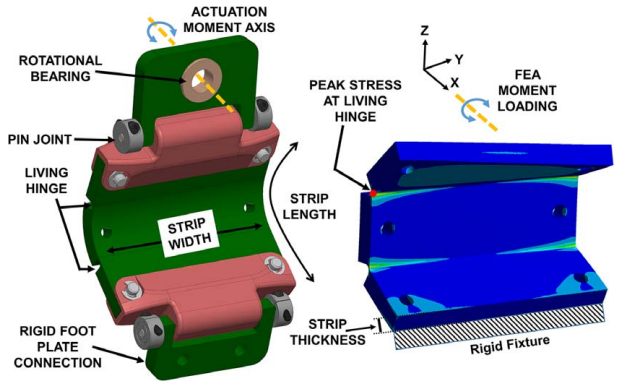

Fig. 7 (Left) CAD of transmission strip and its interfaces and (right) FEA of transmission strip under actuation loading

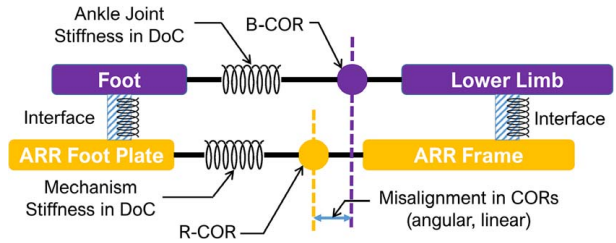

Fig. 8 Conceptual representation of patient's ankle joint and robot mechanisms compliance influences CoR alignment

via a rotational bearing, and the other pin joint has a rigid connection to the foot plate (see Figs. 6 and 7). The foot plate is the interface between the patient's foot and the Flex-ARR. The compliant transmission strips provide the foot plate with 3 DoF with respect to the frame; 2 rotational DoF (INV/EV & PF/DF axis) and 1 translational DoF (along an axis perpendicular to the plane formed by INV/EV and PF/DF axis). In Fig. 6, the axis that intersects the misaligned B-CoR represents a worst-case scenario of misalignment of the patient's PF/DF axis (shown at 5 deg with respect to robot PF/DF axis). Similarly, the B-CoR is misaligned by 9 mm with respect to the R-CoR. These misalignment numbers are based on the literature [17]. The misalignment between the B-CoR and R-CoR can be absorbed by the Flex-ARR DoCs. If there is any misalignment of the CoRs along the Flex-ARR DoFs, the Flex-ARR can be actuated appropriately to minimize or eliminate the misalignment.

Figure 8 shows a schematic of the patient's lower limb and Flex-ARR to highlight potential misalignment. The hashed interfaces represent a mechanical connection (e.g., strap) between the foot plate and the patient's foot and in between the lower limb (above the ankle) and the ARR frame. These interfaces will have some finite stiffness. By connecting the foot to the foot plate, and the leg region to the ARR frame, the ankle is isolated from other lower limb joints to prevent any compensatory motion. In this way, the foot plate and patient's foot move as one with respect to the lower limb and ARR frame. If the B-CoR and R-CoR are misaligned, a reaction load will act on both the ankle joint and ARR mechanism along their DoC directions. If the ARR mechanism's DoC stiffness is much higher than the ankle joint's DoC stiffness, then this reaction load will deform the patient's ankle more than the ARR mechanism, which is highly undesirable. This can cause injury to the patient and compromise their therapy. However, if the mechanism's DoC stiffness is reduced to be lower than the ankle joint's DoC stiffness, the mechanism can deform and absorb misalignment as opposed to the patient's ankle, foot, or lower limb. The mechanism's DoC stiffness cannot be too low or else the deformation of the transmission strips under loading can lead to too much lost motion between the actuators and the foot plate. This motivates the need to optimize the compliant PKM's DoC and DoF stiffness in the Flex-ARR. The detailed design and optimization of transmission strips geometry is discussed in Sec. 6.

6 Detailed Design of Flex-Ankle Rehabilitation Robot System

The detailed computer-aided design (CAD) of the Flex-ARR system can be in seen in Fig. 2, Fig. 6, and Fig. 9. The Flex-ARR system consists of multiple key components: (1) Ground frame, (2) Chair, (3) Alignment tool, (4) Actuator frame, (5) Motor housing, and (6) Mechanism and Foot plate. In Secs. 6.1–6.3, each of the aforementioned components and their functions are discussed in detail. The detailed design includes the Flex-ARR compliant PKM design, Flex-ARR structure and frame, and Flex-ARR actuators and sensors.

6.1 Compliant Parallel Kinematic Mechanism Design. The PKM used in the Flex-ARR includes three transmission strips as shown in Fig. 6—two transmission strips help provide the PF/DF motion and one transmission strip helps provide INV/

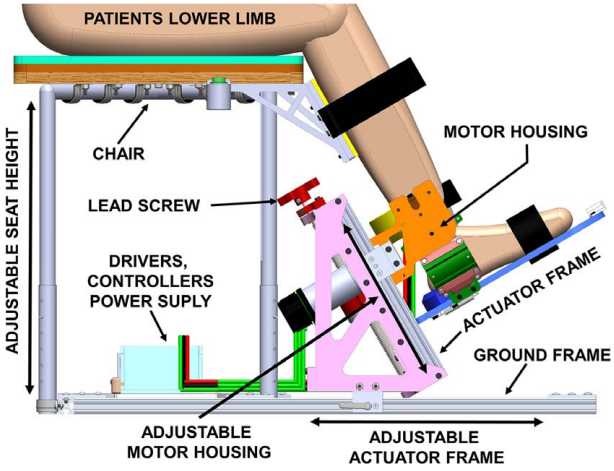

Fig. 9 Flex-ARR system showing all adjustments

EV motion. The details on how this compliant PKM provides the decoupled DoFs and its associated DoCs can be found in the previous study [44]. Using the Flex-ARR CAD, the RoM and other specifications were verified (see Table 2). The transmission strips consist of multiple living hinges, as shown in Fig. 7. These living hinges, which give the transmission strips their rotational DoF about the *Y*-axis and translational DoF along the *Z*-axis, were modeled using existing analytical models of living hinges [47]. As shown in Fig. 7 (left), the transmission strips can bend about their living hinges to accommodate the variations in the height of the ankle malleolus from the foot; most of the population has a height of malleolus between 2.5 and 3.5 in. [42].

During operation, the actuator will apply a moment about the *X*-axis as shown in Fig. 7 (right). Since the transmission strip is curved, the moment applied by the actuator will cause both bending and twisting of the strip about its DoC directions. Using the Euler beam theory, it was determined that the bending stiffness of the transmission strips will be larger than their torsional stiffness since the width of the transmission strip is significantly larger than the thickness. Using ANSYS structural finite element analysis (FEA), the bending and torsional stiffness of the transmission strips was determined. The transmission strips are made from polypropylene copolymer (PP) as it is a common material for living hinges. The material properties for PP copolymer used for analysis were found from the ANSYS Granta material database and MATWEB. As shown in Fig. 7 (right), the transmission strip has a rigid fixture on one end (rigid connection to foot plate), and the maximum actuation moment is applied about the *X*-axis. The geometry was meshed using tetrahedrons with a meshing element size of 0.2 mm.

The compliance of the Flex-ARR PKM was optimized to absorb the misalignment of CoRs noted earlier, without causing large lost motion of the foot plate due to deformation under loading. Also, the dimensions were selected to ensure that the strips do not experience yield failure due to loading. First, FEA was used to optimize the geometry of the transmission strips. For a transmission strip of length 2.7 in. (69 mm), width 3 in. (76 mm), and thickness 0.25 in. (6.4 mm), the bending stiffness was 660 Nm/rad and the torsional stiffness was 30 Nm/rad (while the transmission strip is not curved). This result aligns with our expectations using the Euler beam theory; the bending stiffness is almost 30x of the torsional stiffness. Second, the FEA of a transmission strip in its curved state (as expected while in use) was conducted to ensure it would not yield under loading. The maximum actuation moment will be 25 Nm for PF/DF motion (see Table 2), and this moment will be shared by two transmission strips. Under a maximum actuation moment load of 12.5 Nm, the von-mises stress was highest at the living hinges (see Fig. 7, right) at approximately 109 MPa, which is close to the tensile yield stress of 110 MPa for PP. However, since PP material has a large elongation before failure (elongation at break can be higher than 500%), the stress at the living hinges will be relieved due to strain relief.

To absorb a misalignment between R-CoR and B-CoR in the DoC of the Flex-ARR, stiffness of transmission strip about the *Z*-axis (which is driven by the twisting/torsional stiffness) will determine the reaction torque on the ankle and Flex-ARR. The bending and torsional stiffness's are in series, and the bending stiffness is significantly larger than the torsional stiffness. Hence, for a curved transmission strip (at any expected curvature), the torsional stiffness will decide the DoC stiffness. For a worst-case misalignment of 5 deg in the PF/DF axis of rotation, and misalignment of 9 mm at the CoR, it was determined using CAD that the transmission strips will have to twist (about their *Z*-axis) by approximately 2.5 deg over the maximum RoM of ± 25 deg. Transmission strip twisting by 2.5 deg corresponds to an approximate reaction moment of 1 Nm per strip. This means a total reaction moment of around 2 Nm acts on the patient's ankle. This reaction torque is small (less than 10% of peak passive ankle torque), especially when compared with the reaction torque for a similar angular misalignment for a rigid ARR mechanism. The reaction torque should cause little to no compensatory motion of the knee or hip since the passive stiffness of the knee and hip joint are large (knee passive stiffness is 2x torsional stiffness of transmission strip [48]).

6.2 Flex-ARR Structure and Frame. The Flex-ARR was designed to accommodate physiological variations of the patient's lower limb. As shown in Fig. 9, the height of the chair is adjustable, and the actuator frame can be adjusted toward or away from the chair. The chair relies on discrete adjustments and locks into place using spring pins. The actuator frame moves using linear bearings and uses a brake to lock into place. The motor housing is also adjustable and uses a large pitch lead screw to adjust and lock the motor housing in place. These three adjustments account for the variations in the physical dimensions of the overall lower limb. The compliant transmission strips help account for the variation in malleolus height since the adjustment is along the DoF of the mechanism, which reduces the onerous adjustments for the therapist.

Also, a novel alignment tool and associated mating feature (see Fig. 2) are designed to ensure consistent alignment of the CoRs. In Fig. 10, the alignment tool is shown as worn by a patient before any attachment to Flex-ARR. The alignment tool allows the therapist to locate the B-CoR and use the movable indicator and locking bolt to align the needle of the alignment tool with the B-CoR and lock it into place. In this way, the patients B-CoR is at a fixed known location with respect to the alignment tool mating feature. When the alignment tool mates with the motor housing (see Fig. 2), the B-CoR is reliably collocated with the R-CoR of the Flex-ARR.

6.3 Actuators and Sensors. The Flex-ARR requires two rotary actuators, one for each of the DoFs it provides. Based on the literature, using the passive stiffness of the ankle [40], the required peak torque for PF/DF motion is 25 Nm and for INV/EV motion is 12.5 Nm (see Table 2). In addition, the actuators were chosen to have a reasonably large torque constant to lower the

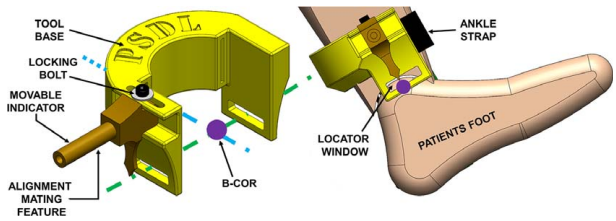

Fig. 10 Flex-ARR alignment tool worn by a patient

motor current (less than 5 A). Maxon Motors EC60 flat motor with a planetary gearhead (GP52C) of transmission ratio of 74:1 was used for PF/DF. Maxon Motors EC60 flat motor with a planetary gearhead (GP52C) of transmission ratio 43:1 was used for INV/EV. The motors can overcome any transmission losses associated with friction in the transmission. Using the motor datasheets and the transmission ratios, the peak output torque and speed at peak torque were determined and shown to meet and exceed the required technical specifications (see Table 2). The motors have incremental encoders that can be used for feedback control, and the encoder count is 4096, which means a position resolution of approximately 0.09 deg.

As discussed earlier, the transmission strips will deform under actuation load, which can create lost motion between the actuators and the foot plate. Given this lost motion (using FEA lost motion under maximum moment load was found to be approximately 5 deg), the motor encoders alone are not adequate for accurate position sensing of the foot plate. Therefore, an IMU is installed on the foot plate (see Fig. 2) to provide additional position information to correct the measurement error due to deformation.

7 Future Work

In this article, the detailed design for a novel ARR (Flex-ARR) is presented, along with all necessary design considerations and discussion of the literature. Future research work will include the overall mechatronic system fabrication, procurement, and assembly. Once assembled, the Flex-ARR's performance will be verified through testing to ensure proper functioning of all safety features and compliance with all design requirements and specifications outlined in Table 2. Verification testing will ensure that subsequent validation testing with human subjects can be performed with no risk. Ultimately, the Flex-ARR performance will be validated with human subject testing. Human subject testing will include evaluating the performance of the Flex-ARR in its various operation modes such as continuous passive motion, resistance training, and assessment modes as such proprioception evaluation. In addition to the sensor-based data, subjective human experience will be captured through survey and interviews of human subjects before, during, and after using the Flex-ARR.

Conflict of Interest

There are no conflicts of interest.

Data Availability Statement

The datasets generated and supporting the findings of this article are obtainable from the corresponding author upon reasonable request.

References

[1] Brockett, C. L., and Chapman, G. J., 2016, "Biomechanics of the Ankle," Orthop. Trauma, **30**(3), pp. 232–238.

[2] Zhang, M., Davies, T., and Xie, S., 2013, "Effectiveness of Robot-Assisted Therapy on Ankle Rehabilitation—A Systematic Review," J. NeuroEngineering Rehabil., **10**(1), p. 30.

[3] Wu, Y.-N., Hwang, M., Ren, Y., Gaebler-Spira, D., and Zhang, L.-Q., 2011, "Combined Passive Stretching and Active Movement Rehabilitation of Lower-Limb Impairments in Children With Cerebral Palsy Using a Portable Robot," Neurorehabil. Neural Repair, **25**(4), pp. 378–385.

[4] Zhang, M., 2016, "Improving Effectiveness of Robot-Assisted Ankle Rehabilitation via Biomechanical Assessment and Interaction Control," Ph.D. thesis, The University of Auckland, Auckland, New Zealand.

[5] Hawson, S. T., 2011, "Physical Therapy and Rehabilitation of the Foot and Ankle in the Athlete," Clin. Podiatr. Med. Surg., **28**(1), pp. 189–201.

[6] Takeuchi, N., and Izumi, S.-I., 2013, "Rehabilitation With Poststroke Motor Recovery: A Review With a Focus on Neural Plasticity," Stroke Res. Treat., **2013**, p. 128641.

[7] Alvarez-Perez, M. G., Garcia-Murillo, M. A., and Cervantes-Sánchez, J. J., 2019, "Robot-Assisted Ankle Rehabilitation: A Review," Disabil. Rehabil. Assist. Technol., **15**(4), pp. 394–408.

[8] Zhang, M., Davies, T. C., Zhang, Y., and Xie, S., 2014, "Reviewing Effectiveness of Ankle Assessment Techniques for Use in Robot-Assisted Therapy," J. Rehabil. Res. Dev., **51**(4), pp. 517–534.

[9] Hancock, G. E., Hepworth, T., and Wembridge, K., 2018, "Accuracy and Reliability of Knee Goniometry Methods," J. Exp. Orthop., **5**(1), p. 46.

[10] Popoff, M., Jourdan, C., Dongas, A., and Schnitzler, A., 2012, "Reliability of Goniometric Measurement of Ankle Dorsiflexion in Hemiparetic Patients," Ann. Phys. Rehabil. Med., **55**(Supplement 1), p. e28.

[11] Spink, M. J., Fotoohabadi, M. R., and Menz, H. B., 2010, "Foot and Ankle Strength Assessment Using Hand-Held Dynamometry: Reliability and Age-Related Differences," Gerontology, **56**(6), pp. 525–532.

[12] Salazar, A. M., Ortega, A. B., Velasco, K. G., and Pliego, A. A., 2018, "Mechatronic Integral Ankle Rehabilitation System: Ankle Rehabilitation Robot, Serious Game, and Facial Expression Recognition System," *Advanced Topics on Computer Vision, Control and Robotics in Mechatronics*, O. O. Vergara Villegas, M. Nandayapa, and I. Soto, eds., Springer International Publishing, Cham, pp. 291–320.

[13] Nurahmi, L., Caro, S., and Solichin, M., 2019, "A Novel Ankle Rehabilitation Device Based on a Reconfigurable 3-RPS Parallel Manipulator," Mech. Mach. Theory, **134**, pp. 135–150.

[14] Saglia, J. A., Dai, J. S., and Caldwell, D. G., 2008, "Geometry and Kinematic Analysis of a Redundantly Actuated Parallel Mechanism That Eliminates Singularities and Improves Dexterity," ASME J. Mech. Des., **130**(12), p. 124501.

[15] Jamwal, P. K., Xie, S. Q., Hussain, S., and Parsons, J. G., 2014, "An Adaptive Wearable Parallel Robot for the Treatment of Ankle Injuries," IEEE/ASME Trans. Mechatron., **19**(1), pp. 64–75.

[16] Jamwal, P. K., Hussain, S., and Xie, S. Q., 2015, "Three-Stage Design Analysis and Multicriteria Optimization of a Parallel Ankle Rehabilitation Robot Using Genetic Algorithm," IEEE Trans. Autom. Sci. Eng., **12**(4), pp. 1433–1446.

[17] Siston, R. A., Daub, A. C., Giori, N. J., Goodman, S. B., and Delp, S. L., 2005, "Evaluation of Methods That Locate the Center of the Ankle for Computer-Assisted Total Knee Arthroplasty," Clin. Orthop., **439**, pp. 129–135.

[18] Alcocer, W., Vela, L., Blanco, A., Gonzalez, J., and Oliver, M., 2012, "Major Trends in the Development of Ankle Rehabilitation Devices," Dyna, **79**(176), pp. 45–55.

[19] Hocoma, n.d., "Lokomat®," www.hocoma.com/solutions/lokomat/, Accessed October 3, 2019.

[20] Girone, M., Burdea, G., Bouzit, M., Popescu, V., and Deutsch, J. E., 2001, "A Stewart Platform-Based System for Ankle Telerehabilitation," Auton. Robots, **10**(2), pp. 203–212.

[21] Li, J., Zuo, S., Zhang, L., Dong, M., Zhang, Z., Tao, C., and Ji, R., 2020, "Mechanical Design and Performance Analysis of a Novel Parallel Robot for Ankle Rehabilitation," ASME. J. Mech. Robot., **12**(5), p. 051007.

[22] Kumar, S., Bongardt, B., Simnofske, M., and Kirchner, F., 2019, "Design and Kinematic Analysis of the Novel Almost Spherical Parallel Mechanism Active Ankle," J. Intell. Robot. Syst., **94**(2), pp. 303–325.

[23] Zhou, Z., Zhou, Y., Wang, N., Gao, F., Wei, K., and Wang, Q., 2015, "A Proprioceptive Neuromuscular Facilitation Integrated Robotic Ankle–Foot System for Post Stroke Rehabilitation," Robot. Auton. Syst., **73**, pp. 111–122.

[24] Wang, C., Fang, Y., Guo, S., and Chen, Y., 2013, "Design and Kinematical Performance Analysis of a 3-RUS/RRR Redundantly Actuated Parallel Mechanism for Ankle Rehabilitation," ASME J. Mech. Robot., **5**(4), pp. 1–11.

[25] Malosio, M., Negri, S. P., Pedrocchi, N., Vicentini, F., Caimmi, M., and Molinari Tosatti, L., 2012, "A Spherical Parallel Three Degrees-of-Freedom Robot for Ankle-Foot Neuro-Rehabilitation," 2012 Annual International Conference of the IEEE Engineering in Medicine and Biology Society, San Diego, CA, Aug. 28–Sept. 1, IEEE.

[26] Yoon, J., and Ryu, J., 2005, "A Novel Reconfigurable Ankle/Foot Rehabilitation Robot," Proceedings of the 2005 IEEE International Conference on Robotics and Automation, Barcelona, Spain, Apr. 18–22.

[27] Liu, G., Gao, J., Yue, H., Zhang, X., and Lu, G., 2006, "Design and Kinematics Analysis of Parallel Robots for Ankle Rehabilitation," 2006 IEEE/RSJ International Conference on Intelligent Robots and Systems, Beijing, China, Oct. 9–15.

[28] Tsoi, Y. H., and Xie, S. Q., 2008, "Design and Control of a Parallel Robot for Ankle Rehabilitation," 2008 15th International Conference on Mechatronics and Machine Vision in Practice, Auckland, New Zealand, Dec. 2–4.

[29] Bi, Z. M., 2013, "Design of a Spherical Parallel Kinematic Machine for Ankle Rehabilitation," Adv. Robot., **27**(2), pp. 121–132.

[30] Lundberg, A., Svensson, O., Nemeth, G., and Selvik, G., 1989, "The Axis of Rotation of the Ankle Joint," J. Bone Joint Surg. Br., **71-B**(1), pp. 94–99.

[31] Barnett, C. H., and Napier, J. R., 1952, "The Axis of Rotation at the Ankle Joint in Man. Its Influence Upon the Form of the Talus and the Mobility of the Fibula," J Anat., **86**(1), pp. 1–9.

[32] Malosio, M., Caimmi, M., Ometto, M., and Tosatti, L. M., 2014, "Ergonomics and Kinematic Compatibility of PKankle, a Fully-Parallel Spherical Robot for Ankle-Foot Rehabilitation," 5th IEEE RAS/EMBS International Conference on Biomedical Robotics and Biomechatronics, São Paulo, Brazil, Aug. 12–15.

[33] Jalgaonkar, N., Kim, A., and Awtar, S., 2020, "Design of an Ankle Rehab Robot With a Compliant Parallel Kinematic Mechanism," ASME International Design Engineering Technical Conferences (IDETC), Virtual Online, Aug. 17–19, pp. 1–10.

[34] Kinetec, n.d., "Kinetec Breva," https://kinetecuk.com/shop/cpm-active/ankle-cpms/kinetec-breva/, Accessed October 3, 2019.

[35] Kinetec., n.d., "Kinetec 5090 Club Foot CPM," https://kinetecuk.com/shop/cpm-active/ankle-cpms/kinetec-5090-club-foot-cpm/, Accessed October 3, 2019.
[36] Chattanooga, n.d., "OptiFlex Ankle CPM," https://www.chattanoogarehab.com/us/optiflex-ankle-cpm-2027, Accessed October 3, 2019.
[37] Biodex Medical Systems, n.d., "System 4 Pro," https://www.biodex.com/physical-medicine/products/dynamometers/system-4-pro, Accessed October 3, 2019.
[38] JACE Systems, n.d., "JACE Ankle A330 CPM," http://www.jacesystems.com/products/ankle/jace_ankle.htm, Accessed October 3, 2019.
[39] Dai, J. S., Zhao, T., and Nester, C., 2004, "Sprained Ankle Physiotherapy Based Mechanism Synthesis and Stiffness Analysis of a Robotic Rehabilitation Device," Auton. Robots, **16**(2), pp. 207–218.
[40] Borges, P. R. T., Santos, T. R. T., Procópio, P. R. S., Chelidonopoulos, J. H. D., Zambelli, R., and Ocarino, J. M., 2017, "Passive Stiffness of the Ankle and Plantar Flexor Muscle Performance After Achilles Tendon Repair: A Cross-Sectional Study," Braz. J. Phys. Ther., **21**(1), pp. 51–57.
[41] Garofolini, A., Taylor, S., McLaughlin, P., Stokes, R., Kusel, M., and Mickle, K. J., 2019, "Repeatability and Accuracy of a Foot Muscle Strength Dynamometer," Med. Eng. Phys., **67**, pp. 102–108.
[42] White, R. M., 1982, *Comparative Anthropometry of the Foot*, Defense Technical Information Center, Fort Belvoir, VA.
[43] Guggenberger, R., Pfirrmann, C. W. A., Koch, P. P., and Buck, F. M., 2014, "Assessment of Lower Limb Length and Alignment by Biplanar Linear Radiography: Comparison With Supine CT and Upright Full-Length Radiography," Am. J. Roentgenol., **202**(2), pp. W161–W167.
[44] Damerla, R., and Awtar, S., 2020, "Constraint-Based Analysis of Parallel Kinematic Articulated Wrist Mechanisms," ASME International Design Engineering Technical Conferences (IDETC), Virtual Online, Aug. 17–19, pp. 1–12.
[45] Awtar, S., Trutna, T. T., Nielsen, J. M., Abani, R., and Geiger, J., 2010, "FlexDex^{TM}: A Minimally Invasive Surgical Tool With Enhanced Dexterity and Intuitive Control," ASME J. Med. Devices, **4**(3), p. 035003.
[46] Awtar, S., and Nielsen, J., 2019, "Parallel Kinematic Mechanisms With Decoupled Rotational Motions," US 10405936B2.
[47] Yong, Y. K., Lu, T.-F., and Handley, D. C., 2008, "Review of Circular Flexure Hinge Design Equations and Derivation of Empirical Formulations," Precis. Eng., **32**(2), pp. 63–70.
[48] Pfeifer, S., Hardegger, M., Vallery, H., List, R., Foresti, M., Riener, R., and Perreault, E. J., 2011, "Model-Based Estimation of Active Knee Stiffness," IEEE International Conference Rehabilitation Robotics, Zurich, Switzerland, June 27–July 1.